# Development of a Global Seismic Risk Model

**Article** *in* Earthquake Spectra · February 2020

DOI: 10.1177/8755293019899953



**18 authors**, including:

Vitor Silva
GEM, EUCENTRE, University of Aveiro
**141** PUBLICATIONS **3,834** CITATIONS
SEE PROFILE

Alejandro Calderon
Global Earthquake Model
**13** PUBLICATIONS **149** CITATIONS
SEE PROFILE

Catarina Costa
GEM
**13** PUBLICATIONS **381** CITATIONS
SEE PROFILE

Jamal Dabbeek
Eucentre, An-Najah National University
**11** PUBLICATIONS **215** CITATIONS
SEE PROFILE

*Article*

EARTHQUAKE SPECTRA

Earthquake Spectra
1–23

DOI: 10.1177/8755293019899953
journals.sagepub.com/home/eqs
SAGE

# Development of a global seismic risk model

**Vitor Silva, M.EERI[1], Desmond Amo-Oduro[1], Alejandro Calderon[1], Catarina Costa[1], Jamal Dabbeek[1], Venetia Despotaki[1], Luis Martins[1], Marco Pagani[1], Anirudh Rao[1], Michele Simionato[1], Daniele Viganò[1], Catalina Yepes-Estrada[1], Ana Acevedo[2], Helen Crowley, M.EERI[3], Nick Horspool[4], Kishor Jaiswal[5], Murray Journeay[6], and Massimiliano Pittore[7]**

**Abstract**

Since 2015, the Global Earthquake Model (GEM) Foundation and its partners have been supporting regional programs and bilateral collaborations to develop an open global earthquake risk model. These efforts led to the development of a repository of probabilistic seismic hazard models, a global exposure dataset comprising structural and occupancy information regarding the residential, commercial and industrial buildings, and a comprehensive set of fragility and vulnerability functions for the most common building classes. These components were used to estimate probabilistic earthquake risk globally using the OpenQuake-engine, an open-source software for seismic hazard and risk analysis. This model allows estimating a number of risk metrics such as annualized average losses or aggregated losses for particular return periods, which are fundamental to the development and implementation of earthquake risk mitigation measures.

**Keywords**

Seismic risk, exposure, vulnerability, seismic hazard, earthquake losses

Date received: 10 December 2019; accepted: 16 December 2019

[1]Global Earthquake Model Foundation, Pavia, Italy
[2]EAFIT University, Medellin, Colombia
[3]EUCENTRE, Pavia, Italy
[4]GNS Science, Wellington, New Zealand
[5]US Geological Survey, Golden, CO, USA
[6]Natural Resources of Canada, Vancouver BC, Canada
[7]GFZ Potsdam, Potsdam, Germany

**Corresponding author:**
Vitor Silva, Global Earthquake Model Foundation, Via Ferrata 1, Pavia 27100, Italy.
Email: vitor.silva@globalquakemodel.org

## Introduction

The first priority of the Sendai Framework for Disaster Risk Reduction (United Nations Office for Disaster Risk Reduction (UNDRR), 2015) is Understanding Risk. Similarly, the United Nations 2030 Agenda for Sustainable Development (United Nations (UN), 2016) proposes 17 goals, 4 of which ask explicitly for a significant decrease in the impact of natural hazards by 2030. The assessment of earthquake risk is the first step toward the development and implementation of measures to mitigate the factors that lead to human and economic losses. Seismic risk information can be used to support decision-makers in the distribution of funds for effective risk mitigation. Between 1992 and 2012, over USD14 billion in funding were provided by the European Union, the Japanese International Cooperation Agency (JICA), the United States Agency for International Development (USAID) and other organizations to prepare for natural hazards (Kellett and Caravani, 2013). At the national scale, after the 2009 M5.9 L'Aquila earthquake, the Italian government invested almost EUR1 billion as part of a 7-year program to reduce earthquake risk (Dolce, 2012). The funding was distributed throughout the administrative regions proportionally to the estimated earthquake risk. Seismic risk assessment can also support the development of financial instruments to transfer the risk from the public sector to the international (re)insurance market (e.g. Turkey, New Zealand, Chile—Franco, 2015), to perform benefit–cost analysis to support retrofitting campaigns (e.g. Colombia—Mora et al., 2015) or to design long-term risk reduction plans (e.g. Istanbul—Erdik and Durukal, 2008).

Prior to the 1960s, underwriters at property insurance companies would use pin maps to check for concentrations of their exposure for perils such as fire, lightning, and wind storms. This approach, being very time intensive, was eventually abandoned, and the absence of a major earthquake since 1906 from the insurance perspective led to a general sense of complacency. Primary insurers either purchased reinsurance for their exposures at risk based on crude heuristics or decided to forgo reinsurance altogether. The 1989 Loma Prieta earthquake, the 1994 Northridge earthquake, and the 1995 Kobe earthquake served as rude shocks to the industry and contributed in part to the adoption of earthquake risk models to improve the understanding and management of property exposure to catastrophic events (Kozlowski and Mathewson, 1995).

Despite the recognition of the importance of risk information, probabilistic seismic risk models at the national or subnational level are still scarce and unfortunately only openly available for a few regions (e.g. Crowley et al., 2009; Jaiswal et al., 2015; Salgado-Gálvez et al., 2013; Silva et al., 2014a). Some of the reasons behind this paucity of risk models include the lack of probabilistic seismic hazard models, insufficient data concerning the built-environment, lack of adequate vulnerability functions, and insufficient local capacity to perform complex hazard and risk analyses. As a response to this challenge, the Global Earthquake Model (GEM) Foundation in collaboration with its partners led a 4-year effort to produce a global seismic risk model, whose results were released in December 2018 (www.globalquakemodel.org/gem). This effort also benefited from various models, datasets, and technical reports produced as part of the first phase of GEM (2009–2013). Additional information about these products can be found at www.globalquakemodel.org/publications.

The GEM global model comprises a mosaic of individual risk models, which were produced as part of regional programs or bilateral collaborations between GEM and national institutions (e.g. the U.S. Geological Survey (USGS) and Federal Emergency Management Agency (FEMA) in the United States, Natural Resources Canada (NRCan) in Canada,

GNS Science in New Zealand). Each risk model has three main components: (1) an exposure model defining the spatial distribution, replacement cost, and vulnerability class of the residential, industrial, and commercial building stock, (2) a suite of vulnerability/fragility functions to estimate the likelihood of damage/loss conditioned on a set of ground shaking intensity measure (IM) levels, and (3) a probabilistic seismic hazard analysis (PSHA) model characterizing the probability of exceeding given levels of ground shaking in the region within a specific time span. The seismic risk analyses were performed using the OpenQuake-engine, the open-source platform for seismic hazard and risk analysis, supported by GEM (Pagani et al., 2014; Silva et al., 2014b). The analyses results include estimates of annualized average losses, probable maximum losses (for a set of return periods), loss exceedance curves for each occupancy (i.e. residential, commercial, and industrial), and earthquake risk maps. The economic losses presented herein are only due to direct physical damage caused by ground shaking on the residential, commercial, and industrial buildings. Losses due to damage in governmental facilities, healthcare infrastructure, lifelines, or educational buildings were not considered, nor any potential losses due to business interruption and other systemic or cascading effects. Furthermore, secondary hazards such as liquefaction, landslides, and tsunamis were not considered.

This study presents an overview of the main components of the global seismic risk model and discusses the main findings at the global scale. Additional information about the risk assessment methodology and detailed risk metrics for specific regions and countries can be found in other publications, as mentioned in the following sections.

## Global, regional, and national initiatives on seismic risk modeling

The period from 1990 to 1999 was decreed by the United Nations as the International Decade for Natural Disaster Reduction (IDNDR), propelling many initiatives to improve the understanding of earthquake hazard and risk. Arguably, the most relevant was the Global Seismic Hazard Assessment Program (GSHAP—Giardini, 1999), which combined several national and regional models to produce the first global hazard map of peak ground acceleration for a return period of 475 years on rock. This map has been one of the main references to illustrate the threat posed by earthquakes globally. Li et al. (2015) combined the GSHAP hazard map with empirical vulnerability functions, population density information, and social wealth data to estimate human and economic losses globally. On another initiative, since 2009, the United Nations International Strategy for Disaster Risk Reduction (UNISDR) has been supporting the development of the Global Assessment Report (GAR, 2009, 2015), one of the most notable efforts at the global scale to provide uniform average annual losses (AALs) and probable maximum losses for multiple hazards. The exposure model used by GAR was derived based on a top-down approach, where national/regional population, socioeconomic data and building-type information were used as proxies to estimate the spatial distribution of building counts (DeBono and Chatenoux, 2015). For the hazard component, a fully probabilistic model was developed using the NEIC-USGS earthquake catalog and hundreds of seismic sources distributed across six tectonic regions (Ordaz et al., 2014). This was one of the first attempts to model seismic hazard at the global scale using a homogeneous procedure, resulting in sets of hazard curves and earthquake scenarios. These scenarios were used to estimate annualized average losses and aggregated losses for specific return periods.

In recent years, there were also a number of projects that aimed at assessing earthquake risk at the national, subnational, or urban scale. These initiatives in general shared a

similar structure. A probabilistic seismic hazard model was developed based on the best available fault data and instrumental/historical earthquake catalogs, magnitude–frequency distributions were defined for a number of seismogenic sources, and sensitivity analyses were performed to identify which ground motion predictions equations (GMPEs) should be incorporated within a logic tree structure for each tectonic region (e.g. Europe—Woessner et al., 2015; Africa—Poggi et al., 2017; Middle East—Giardini et al., 2018). The exposure datasets were defined based on national housing censuses (e.g. South America—Yepes-Estrada et al., 2017), cadastral databases (e.g. Medellin—Acevedo et al., 2017) or through a combination of locally collected data and satellite imagery (Central Asia—Wieland et al., 2015). These exposure datasets usually provide the distribution of the number of buildings, replacement cost, number of occupants, and vulnerability classes at the smallest available administrative level, or on a grid (whose spacing might be either evenly spaced or inversely proportional to the expected building density—Pittore et al., 2020). For the vulnerability component, due to the need to cover a wide variety of building classes in regions that might not have sufficient damage data, an analytical approach was often followed. In this process, numerical models representing the structural capacity of each building class are tested against large sets of ground motion records using either nonlinear static procedures (Campos Costa et al., 2010) or time history analysis (e.g. Villar-Vega et al., 2016). A suite of fragility functions defining the probability of exceeding a number of damage states conditioned on a given intensity measure (e.g. PGA, SA) was developed and then converted into vulnerability functions (e.g. probability of loss ratio conditional on an intensity measure) using a damage-to-loss model (i.e. relation between the physical damage state and the probabilistic distribution of loss ratio—Yepes-Estrada et al., 2016). The seismic risk metrics produced by these regional initiatives include average annualized losses, exceedance probability curves, and risk maps for specific return periods (e.g. Crowley et al., 2018).

At the national level, it is also relevant to mention a number of efforts that either contributed directly to the global seismic risk model presented herein or were fundamental for the validation of the risk results. These include studies for Turkey (Bommer et al., 2002), Italy (Crowley et al., 2009), Portugal (Silva et al., 2014a), the United States (Jaiswal et al., 2015), New Zealand (Horspool and King, 2017), Iran (Motamed et al., 2018), and Costa Rica (Calderon and Silva, 2018).

## Global seismic hazard modeling

The seismic hazard component of the global risk model is a mosaic of regional (e.g. South and Central America, Central Asia, Sub-Saharan Africa, Europe) as well as national (e.g. Canada, United States, Indonesia, Australia, New Zealand, Philippines, South Africa) earthquake hazard models, called the GEM mosaic. The national maps produced by agencies that are officially mandated by their respective governments to develop or to update seismic hazard information for their country were preferred. A minor fraction of the GEM mosaic (2018.1 version) contains models that are not necessarily recognized or endorsed by the government entities, but are simply available through the peer-reviewed literature (e.g. India—Nath and Thingbaijam, 2012), or developed internally at the GEM secretariat (e.g. Russia, Pacific Islands). The mosaic thus incorporates a number of openly available probabilistic seismic hazard assessment (PSHA) models, which can support seismic risk assessment. All of these models are described using a standard data format, compatible with GEM's OpenQuake-engine (Pagani et al., 2014). This format was designed to be sufficiently flexible to cope with probabilistic seismic hazard models developed using different

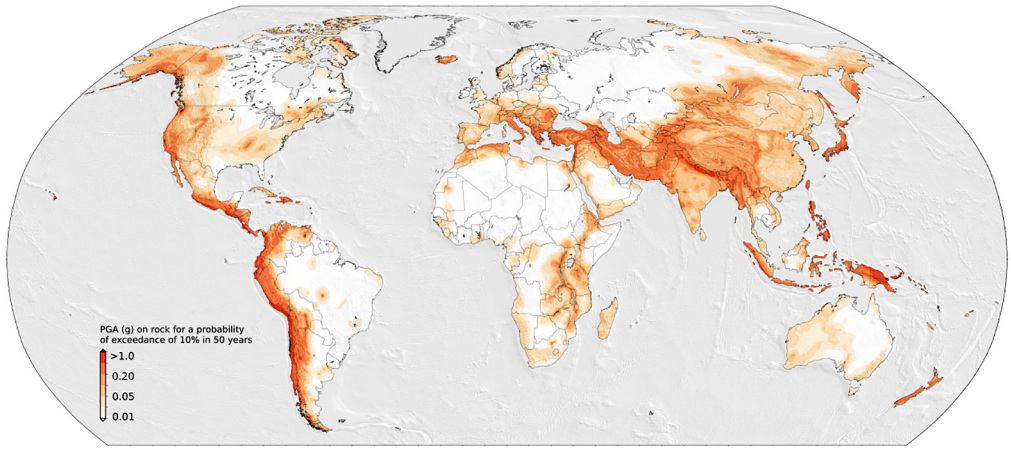


**Figure 1.** Global seismic hazard map (version 2018.1) representing peak ground acceleration (in g) for a probability of exceedance of 10% in 50 years (equivalent to the 475 year return period) on rock (Pagani et al., 2020—https://maps.openquake.org/map/global-seismic-hazard-map).

software/tools representing hazard characterization of various tectonic regions of the world. Such a large compilation of hazard data/models allows a vast spectrum of hazard and risk analyses to be performed and enables a more comprehensive comparison between the main characteristics of the various models (see Pagani et al., 2016 for an example of comparisons using the models for Japan, New Zealand, and Taiwan). Figure 1 illustrates the global seismic hazard map in terms of peak ground acceleration (PGA, as a fraction of g) for a probability of exceedance of 10% in 50 years (equivalent to a 475-year return period) on rock. A detailed description of how the global hazard model was developed can be found in Pagani et al. (2020).

## Global exposure modeling

The exposure model used in the seismic risk assessment comprises information regarding the number of buildings, geographical location, replacement costs (structural, nonstructural, and contents), number of occupants and vulnerability classes of the residential, commercial, and industrial building stock. The derivation method for the residential building stock differed considerably from the commercial and industrial counterpart. For the former occupancy, the latest building housing census of each country was used to estimate the number of buildings distributed across a set of building classes, with the exception of Central Asia, United States, New Zealand, and Australia, for which an exposure dataset already existed (Federal Emergency Management Agency (FEMA), 2012; Dunford and Power, 2014; Pittore et al., 2020). For the commercial and industrial building stock, socioeconomic data ranging from the work force (across all sectors) and industry built-up area to the number of enterprises and offices were collected and combined with a mapping scheme to estimate the expected number of commercial and industrial buildings. For the purposes of this model, commercial buildings comprise retail and wholesale stores, hotels, repair services, restaurants, and offices, while industrial facilities cover manufacturing (paper, plastic, textiles, food, drugs, vehicles) and mining. In general, the derivation procedure followed the steps described in the following:

1. Estimation of the number of buildings based on the housing census for the residential building stock or socioeconomic data for the commercial and industrial facilities (e.g. Motamed et al., 2018).
2. Allocation of each asset into a building class using a mapping scheme. These mapping schemes establish the relation between a number of attributes from the census survey (e.g. main material of construction, date of construction) or type of activity (e.g. offices, warehouses) and one or multiple building classes (e.g. Yepes-Estrada et al., 2017). All building classes have been defined according to an updated version of the GEM taxonomy (Brzev et al., 2013).
3. Definition of the average built-up area per building class or occupancy type. The built-up area for the residential buildings represents all living areas, and average values are usually provided by the National Statistical Offices. The average built-up area for industrial and commercial buildings was estimated from satellite imagery and building footprints from *OpenStreetMap*. This step allows calculating the total area of each building class per administrative area (e.g. Dabbeek and Silva, 2019).
4. Definition of the average replacement cost per building class (i.e. reinforced concrete is usually more expensive than masonry) and type of area (i.e. prices are higher in urban areas and lower in rural areas). The replacement costs were estimated on the basis of rebuilding the destroyed or damaged assets with improved quality (following the "building back better" concept), and not the pre-disaster costs. The replacement costs have been adjusted to the year 2017.

The exposure data were defined at the smallest available administrative level for each country, unless the geographical extension of the administrative areas was too large. For those cases (e.g. Ethiopia, South Sudan, Tanzania), to avoid an over-aggregation of the assets at a single location and consequently a poor estimation of the site-to-source distance (e.g. Bazzurro and Park, 2007), the assets were spatially disaggregated at a fine resolution based on the population density provided by WorldPop (Lloyd et al., 2017) and the night time lights (Elvidge et al., 2012). It is recognized that the development of exposure models is affected by several aleatory and epistemic uncertainties (e.g. cost per square meter, area per dwelling or facility, number of dwellings per building, definition of the mapping schemes). In the current version of the global risk model, none of these uncertainties have been propagated to the risk results, and instead only mean values have been used. The exploration of the impact of these sources of uncertainty in seismic risk assessment is part of the future developments.

The presentation of exposure data at the global scale presents several challenges due to the disparity in the geographic size of the administrative divisions between different countries. To minimize this issue, we have spatially disaggregated the number of buildings on an evenly spaced grid with $30 \times 30$ arcsecs using the same auxiliary datasets previously mentioned and then aggregated them on a hexagonal grid with a spatial resolution of $0.30 \times 0.34$ decimal degrees (approximately 1000 $km^2$ at the Equator), as depicted in Figure 2. Resolutions smaller than this complicate the identification of rural areas or small urban centers, while coarser resolutions will merge nearby cities or adjacent small countries.

The global exposure model contains 1.3 billion residential, 90.9 million commercial, and 35.5 million industrial buildings, with an aggregated replacement cost of USD203.6 trillion. Most of the total cost (76%) is distributed across 15 countries, as presented in Figure 3.

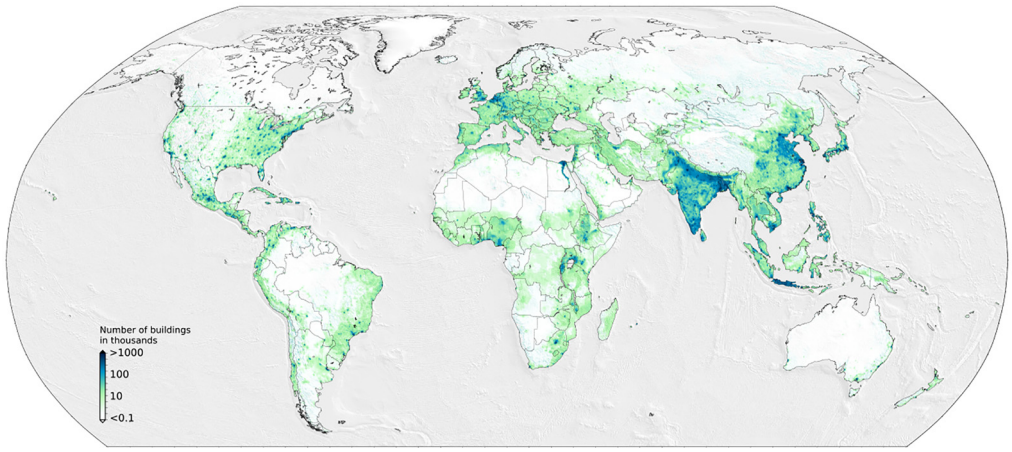


**Figure 2.** Global exposure map in terms of the number of residential, commercial, and industrial buildings at a hexagonal grid with a 0.30 × 0.34 decimal degrees spatial resolution (https://maps.openquake.org/map/global-exposure-map).

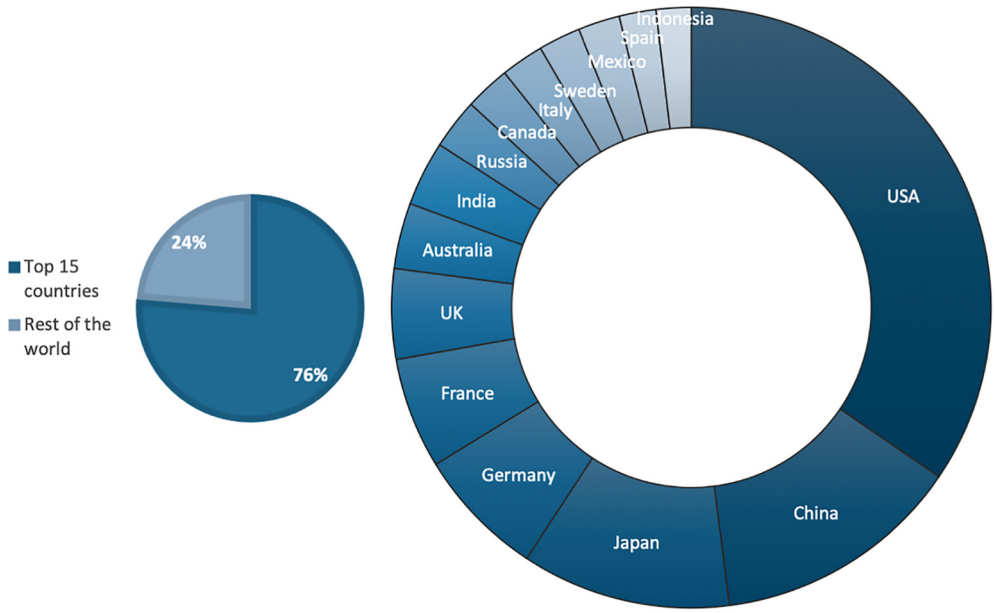


**Figure 3.** Relative contribution to the aggregated replacement cost of the top 15 countries with the global replacement cost (left) and relative replacement cost of the top 15 countries (right).

The seismic vulnerability of the global building stock was classified into 260 building classes. The most common types of construction (in terms of the number of buildings) are unreinforced masonry (27%), wooden or bamboo (21%) and reinforced concrete (18%). Confined or reinforced masonry, mixed types (usually combination of masonry with

wood), and adobe/earthen represent 11%, 10%, and 7%, respectively. Steel represents 2% and other construction types (usually used for informal construction and comprising light materials such as metal sheets, plastic, or vegetative materials) represent 4% of the global building stock. In contrast, the construction classes that account for almost 90% of the total replacement cost are reinforced concrete (34%), wooden or bamboo (27%), unreinforced masonry (18%), and steel (10%). Confined or reinforced masonry, mixed types, adobe/earthen, and other construction types represent 7%, 2%, 1%, and 1% of the total replacement cost, respectively.

## Seismic vulnerability modeling

Despite some regional efforts to develop uniform sets of fragility and vulnerability functions for national and regional seismic risk analysis (e.g. Romao et al. 2019 in Europe, Villar-Vega et al., 2016 in South America), at the global scale the availability of these functions is still insufficient to represent all of the different types of construction, especially in the context of the developing world (Yepes-Estrada et al., 2016), or regions where destructive earthquakes are rare. Moreover, with a few exceptions, most of the existing vulnerability functions have not been tested against damage data from previous events or have not been applied within a probabilistic framework for earthquake loss assessment (Villar-Vega and Silva, 2017). To overcome (or at least minimize) some of these issues, a repository of vulnerability functions for the most common building classes was developed, using a uniform approach (Martins and Silva, 2018). In general, the derivation procedure followed the steps described in the following:

1. Identification of the most common building classes in the region, using peer-reviewed literature, WHE reports, and web surveys (https://platform.openquake.org/building-class/).
2. Definition of the structural and dynamic properties of each building class (e.g. yield and ultimate drifts, elastic and yield period of the first mode of vibration, participation factor of the first mode of vibration, common failure mechanisms). These attributes were collected from the literature (e.g. numerical studies, experimental tests, expert judgment, damage observations).
3. Development of representative equivalent single-degree-of-freedom (SDOF) oscillator for each building class (using the parameters identified in Step 2), using the *pinching4* model from the open-source package for structural analysis OpenSees (McKenna et al., 2000).
4. Selection of ground motion records using strong motion databases from the United States, Japan, Chile, Mexico, and Europe. The use of a large set of time histories aimed at propagating the record-to-record variability to the vulnerability assessment.
5. Performing nonlinear time history analysis to evaluate the structural response (i.e. engineering demand parameter (EDP)—maximum displacement and acceleration) of the SDOF oscillators against the selected ground motion records. This step uses OpenSees (McKenna et al., 2000) to estimate the structural response, and the Risk Modelers Toolkit developed by GEM to compute the fragility functions.
6. Estimation of the probability of exceeding a set of damage states (slight, moderate, extensive and complete damage) using cloud analysis (Jalayer and Cornell, 2002), and a damage criterion based on the yielding and ultimate displacement points (e.g. Villar-Vega et al., 2016). Figure 4 illustrates the fragility functions for two of

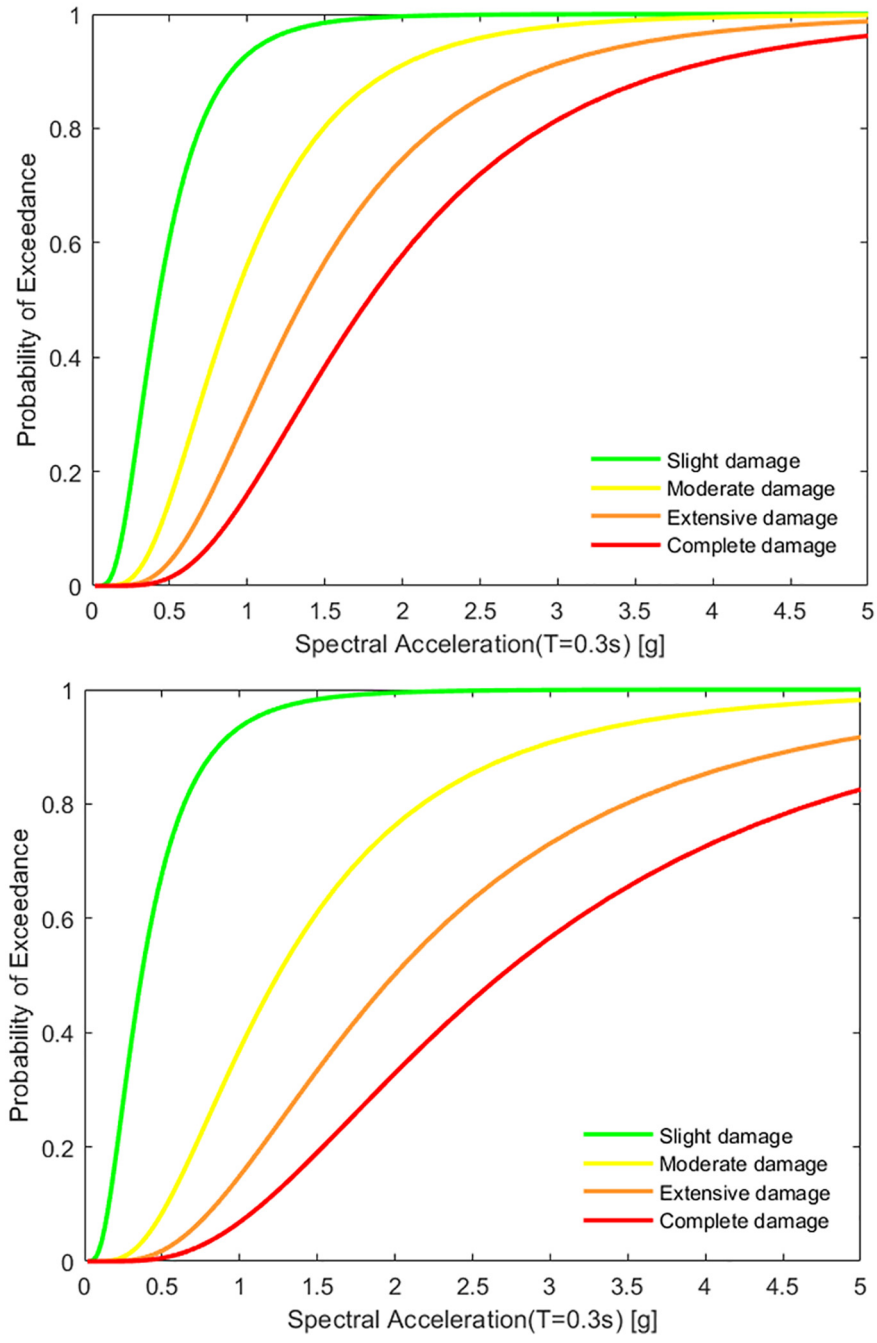


**Figure 4.** Fragility curves for unreinforced masonry with 2 stories (left) and reinforced concrete (right) buildings with 3 stories, two of the most common building classes around the world (Martins and Silva, 2018).

the most common building classes in the global exposure model: unreinforced masonry with 2 stories and moment-frames reinforced concrete with 3 stories and low ductility.

7. The fragility functions were converted into vulnerability functions (i.e. probability of loss ratio conditional on ground shaking) using a damage-to-loss model (e.g. Yepes-Estrada et al., 2016). These functions were used directly in the assessment of economic losses.

This procedure allows propagating the main four sources of uncertainty in fragility and vulnerability assessment: record-to-record, building-to-building, damage criterion, and damage-to-loss variability. Therefore, each loss ratio in the vulnerability functions is modeled using a beta distribution with a mean and coefficient of variation. For the sake of simplicity, in this version of the global risk model only the mean loss ratios were used in the risk analyses. The fragility functions were tested against damage observations from past events (e.g. Villar-Vega and Silva, 2017), using damage data from the literature (e.g. Pomonis, 2002; Daniell et al., 2011) and the National Oceanic and Atmospheric Administration (NOAA) disaster database. In this verification, we evaluated whether the observed failure mechanisms were reproduced and whether the estimated distribution of the damage across the existing building classes was in agreement with the observations (Villar-Vega and Silva, 2017). The same process was followed to test the vulnerability functions using loss data from the NatCatService database (MunichRe, 2019).

## Seismic risk assessment

### *Methodology*

The estimation of the earthquake risk was performed using the event-based probabilistic risk assessment calculator of the OpenQuake-engine. In this calculator, the PSHA model is used to create an earthquake rupture forecast (i.e. list of all of the possible ruptures that can occur in the region of interest with the associated probability of occurrence in a given time span), which is then employed to generate stochastic event sets (SES). Figure 5 depicts 50 event sets at the global scale, each one with a 1 year time span. Due to the random

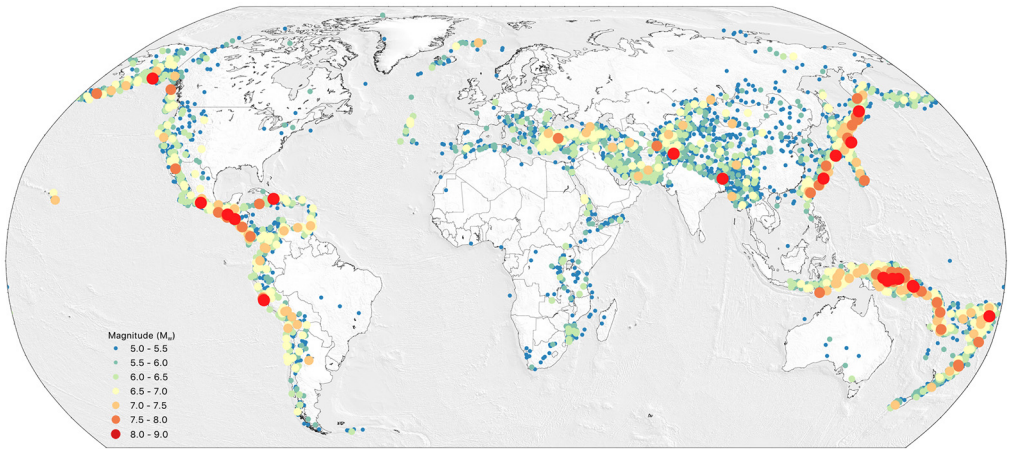


**Figure 5.** Example of a stochastic event set (for a time span of 50 years) using the Global Hazard Model by Pagani et al. (2020).

nature of this process, a large number of SES is required in order to reach statistical convergence in both the seismic hazard and risk assessments (Silva, 2017). In this process, the epistemic uncertainty in the seismogenic model is propagated through the use of logic trees (Pagani et al., 2014).

For each event in the SES, a ground motion field is generated, considering one or multiple GMPEs associated with the respective tectonic region. The intra- and inter-event aleatory variability from the GMPEs are propagated using a Monte Carlo approach, and the spatial correlation in the ground motion residuals from the same *IM* can be considered using the correlation model from Jayaram and Baker (2010). Site conditions are taken into account using average shear wave velocity within the top 30 m layer ($V_{S30}$), estimated using the simplified approach by Wald and Allen (2007). The authors recognize the limitations in employing topographic slope to infer VS30 values, but for large-scale risk assessment, it is arguably the only methodology capable of providing, on average, reasonable results (e.g. Lemoine et al., 2012). It should also be noted that countries such as Australia, Colombia, and Portugal have national VS30 maps which rely not only on topography but also on geological maps and can thus enable a better consideration of site effects.

The computed ground shaking at the location of each asset is combined with the associated vulnerability function and replacement cost to compute the expected loss for each event in the SES. This allowed the derivation of event loss tables, comprising the losses per asset for each event in the SES. These tables were then used for the calculation of several risk metrics, including exceedance probability curves and average annualized losses (Silva et al., 2014a). The former metric expresses the rate of exceeding ($\lambda$) a given loss $l$, as described by Equation 1

$$\lambda(L>l) = \frac{1}{n}\sum_{i=1}^{k} I(L_i>l) \tag{1}$$

where $I(L_i>l)$ is a function equal to 1 when $L_i>l$, $k$ is the total number of events, $L_i$ stands for the loss caused by event $i$, and $n$ represents the number of 1 year SES. Likewise, the $AAL$ can be computed using the following equation

$$AAL = \frac{1}{n}\sum_{i=1}^{k} L_i \tag{2}$$

These metrics are calculated for each branch of the logic tree, leading to a probabilistic distribution of risk. For the purposes of communicating the results of the global risk model, only mean values across all branches are presented. Moreover, the main findings and risk maps are expressed in terms of $AAL$, but other results such as exceedance probability curves and aggregated losses for specific return periods can be found in the country profiles on the Global Risk Model Explorer (https://maps.openquake.org/map/global-seismic-risk-map). It is relevant to note that the calculation of $AAL$ is also possible through fully analytical approaches (e.g. Salgado-Gálvez et al., 2013; Silva et al., 2014a), similar to the current practice in seismic hazard assessment (i.e. Classical PSHA—Cornell, 1968). The analytical approach does not require the Monte Carlo sampling process which is often computationally demanding, but it does not allow the calculation of probable maximum losses considering both the spatial correlation in the ground motion residuals and the

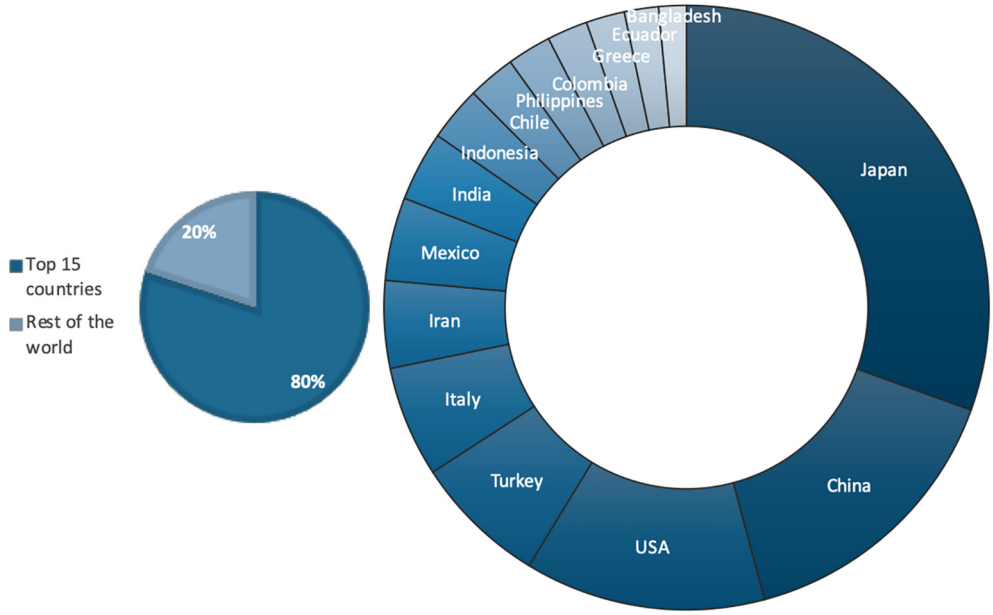


**Figure 6.** Relative contribution to the global AAL of the 15 countries with the highest *AAL* (left) and relative *AAL* of the top 15 countries (right).

correlation in the seismic vulnerability. Comparisons between both approaches can be found in Silva (2017).

## Results

Following the methodology discussed in previous section, 20,000 event sets were generated for each logic tree branch, leading to more than 140M events with magnitude greater than M5.5. AALs were calculated at the smallest available administrative division of each country and then aggregated at the national level in order to compare risk across all countries. The global risk model indicates a global AAL of USD45 billion, with only 15 countries contributing to 80% of this value, as illustrated in Figure 6. The results presented herein are further discussed in the following section.

As expected, the rank presented in Figure 6 is led by countries with a large building portfolio with relatively high construction costs, located in areas with moderate-to-high seismic hazard. Such criterion to rank countries in terms of their relative seismic risk will naturally exclude smaller nations, despite the fact that a great portion of their population or gross domestic product (GDP) might be exposed to high levels of risk. Two alternative criteria are presented herein to compare risk between countries. In the first approach, the *AALs* are normalized by the construction cost per square meter, thus disregarding the fact that the same building will have different replacement costs depending on the country. These results are presented in Figure 7 following the same style.

This ranking highlights countries with a large number of buildings located in regions with moderate to high seismic hazard. Due to the normalization of the *AAL* (in USD) based on the construction cost per square meter (in USD/$m^2$), in practice this indicator

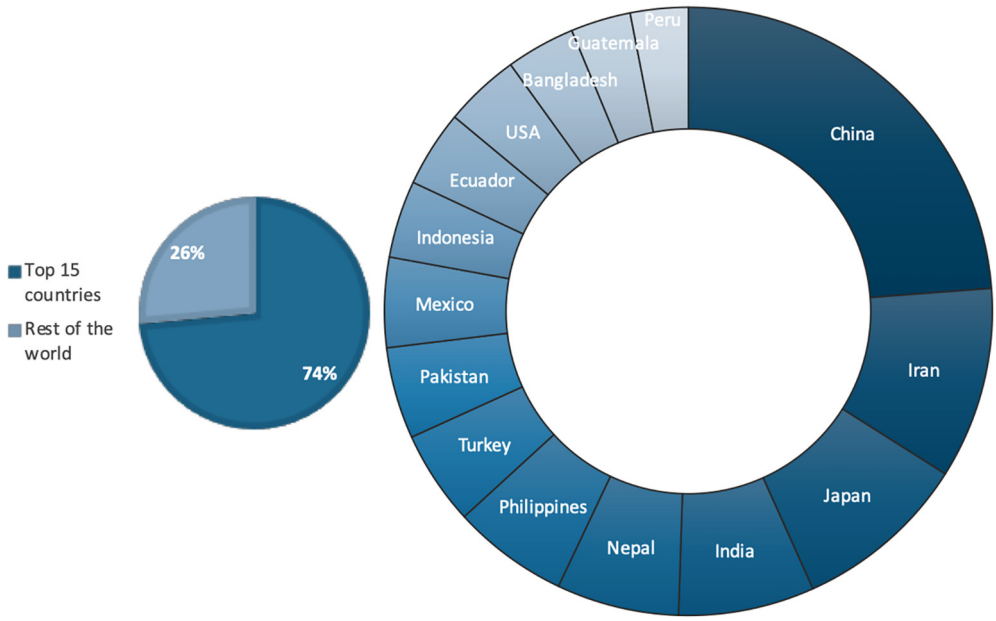


**Figure 7.** Relative contribution to the global normalized AAL of the 15 countries with the highest *AAL* (left) and relative normalized *AAL* of the top 15 countries (right).

represents the built-up area (in $m^2$) that is lost on average per year. In this case, the top 15 countries contribute with 74% of the AAL of built up 62 million $m^2$. Finally, the *AALs* were also divided by the total replacement cost of the building stock of each country, leading to an AAL ratio (*AALR*). The *AALR* highlights countries with a relatively small geographical area and with a vulnerable building stock, as large countries are unlikely to have their entire territory exposed to moderate or high seismic hazard. Other criteria can be explored to compare earthquake risk between various countries, such as the normalization based on the GDP or the national capital stock (e.g. World Bank, 2017). The results for the top 15 countries are presented in Figure 8.

It is interesting to evaluate which building classes are contributing the most to the global *AAL*. The current model indicates that reinforced concrete, unreinforced masonry, and wooden structures represent 36%, 18%, and 16% of the global *AAL*, respectively. The reason for the high contribution of reinforced concrete is its higher construction cost and common use in regions with moderate to high seismic hazard (e.g. Japan, China, Middle East). Unreinforced masonry, although also frequently used in regions of low seismic hazard (e.g. northern Europe, Africa), is a type of construction characterized by a high seismic vulnerability (see Figure 4). For some regions (e.g. Central America and the Caribbean), unreinforced masonry is responsible for more than 25% of the *AAL*. Finally, wooden structures are also particularly common in countries with high seismic hazard (e.g. United States, Chile, Japan).

The evaluation of the spatial distribution of earthquake risk at the subnational level allows the regions contributing the most to the national risk to be identified and thus where risk reduction measures should be prioritized. For the arguments described in the

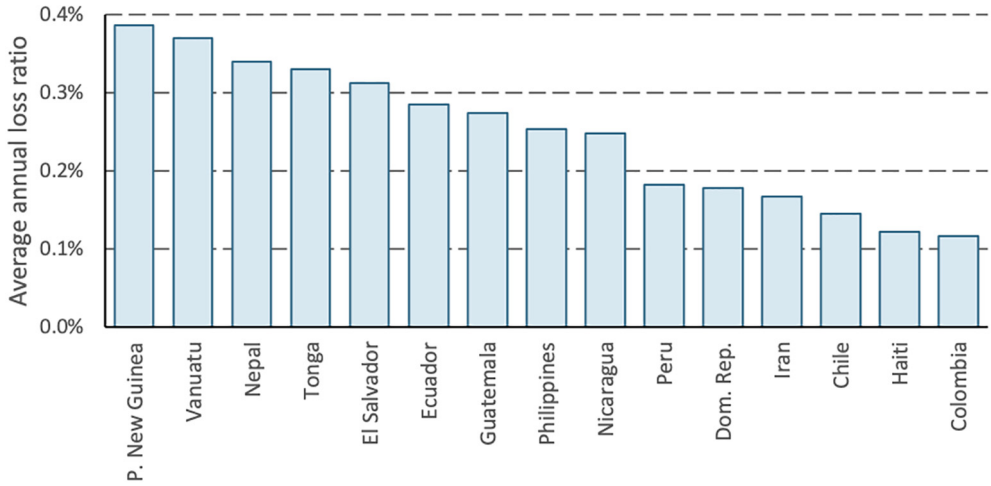


**Figure 8.** Top 15 countries in terms of the highest Average annual loss ratios (in percentage).

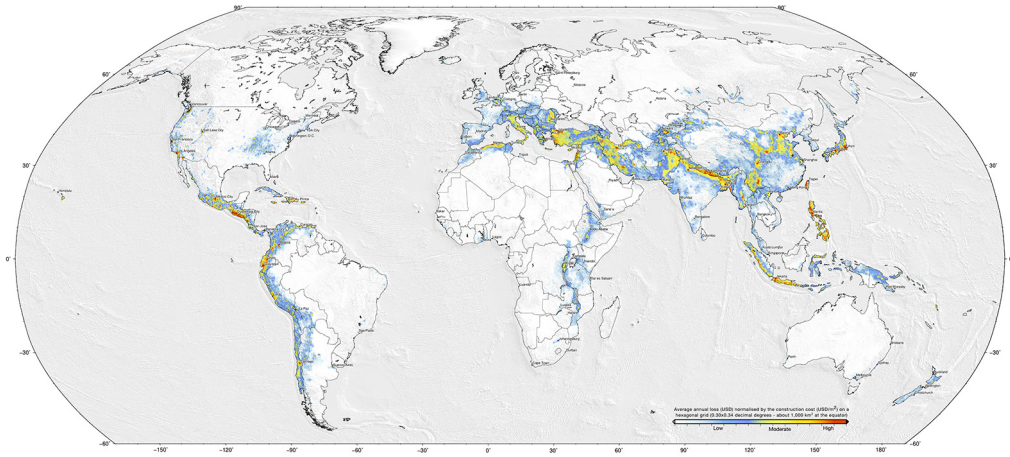

**Figure 9.** Global distribution of average annual losses normalized by the construction cost per unit of area (USD/USD.m2) at a hexagonal grid with a 0.30 × 0.34 decimal degrees spatial resolution (https://maps.openquake.org/map/global-seismic-risk-map).

global exposure modeling section, it is useful to map earthquake risk using a uniform grid. Moreover, due to the large differences between the replacement costs across all countries (e.g. costs per square meter of masonry in Switzerland are one order of magnitude above the costs in rural areas in Albania for similar construction), normalizing the AALs based on the construction costs is also considered. The results at the global scale using this approach are illustrated in Figure 9.

As expected, the nature and extent of the underlying seismic hazard remains the main driver behind the high seismic risk for most parts of the world. Also, the level of risk gets

aggravated when such hazard is faced by a vulnerable population and building stock. The areas with highest earthquake hazard combined with a high concentration of vulnerable population and built environment are shown to possess the highest seismic risk (all shown in warm colors). In particular, the subduction zone of South and Central America along the entire Pacific border from Chile to the Caribbean coast of Colombia and Venezuela and through Southern Mexico shows very high risk. Similarly, another very active plate boundary region with large population exposure and earthquake risk is that of the Australia-Pacific plate boundary region covering Indonesia and most of southeast Asia. Most of Central Asia exhibits high earthquake hazard and has already witnessed several deadly earthquakes in the recent past that have led to large number of casualties and economic losses. Countries in southern Europe (Italy, Greece) and parts of northwestern Africa (Algeria, Morocco) along with much of the Middle East face high risk given the high concentration of population and the complex interaction between four major tectonic plates. Both China and India, being the two most populated countries with over 36% of total world population also face high earthquake hazards (mainly from the collision of the India and Eurasia plates at the Main Frontal Thrust along most of Himalayas for India, which is extended farther along the northeastern India and parts of China through multiple complex fault systems) and risk. Interestingly, not all the areas that show broad swath of high hazard in these countries also show an equivalent level of high risk everywhere. Risk is a confluence of a hazard with the vulnerability of built environment exposed to that hazard; thus, vulnerability plays a significant role by identifying and pinpointing the hotspots within each of the high hazard zones. Clearly, most of the world's earthquake risk now appears to be highly concentrated along a dozen or so large urban population centers, all highlighted with yellow through red colors as areas of moderate and high earthquake risk. It is worth noting that the areas shown with low seismic risk (green or blue colors) in the map do not necessarily reflect that these countries would never experience damaging events in the future. It is simply portraying the fact that the relative likelihood of such phenomena is low when directly compared with other seismically active regions of the world.

## *Discussion of results*

As previously mentioned, the economic losses presented in this study are only due to direct physical damage caused by ground shaking, and therefore, the possible effects due to secondary hazards such as liquefaction, landslides and tsunamis were not considered. Although it has been observed that ground shaking is frequently responsible for the majority of the damage (Daniell et al., 2017), the consideration of other phenomena and building occupancies would have certainly increased the values presented herein.

Throughout the development of the global seismic risk model, various components were subjected to verification and validation exercises. These include the incorporation of comments and suggestions from experts from dozens of countries solicited through workshops over 4 years (e.g. Addis Ababa, Pavia, Bishkek, Gandhinagar, Kathmandu, Lima, Medellin, San Jose, Santo Domingo), the testing of the fragility and vulnerability datasets against loss data from past events, and the comparison of the average annualized losses provided by other initiatives. Most local experts advised on updating and/or improving exposure data and mapping schemes, in which the list of building classes, associated fractions, and replacements costs were adjusted. The fragility and vulnerability functions were tested using damage and loss data from 123 past events between 1980 and 2017. Although many more destructive events occurred within this period, we only considered events for

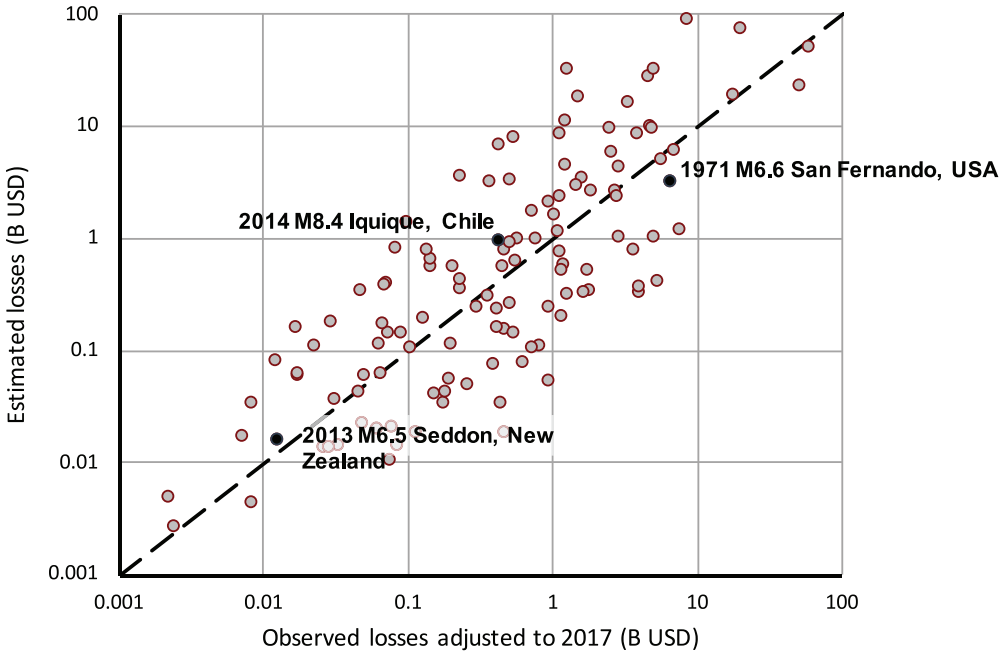


**Figure 10.** Comparison between estimated and observed losses for 123 past events (1980-2017).

which it was possible to obtain damage and loss estimates with a reasonable level of confidence. Additional verifications using damage and loss observations from past events are part of the current phase of GEM (2019–2021).

In this process, USGS *ShakeMaps* were used with the global exposure dataset and the previously described fragility and vulnerability functions to estimate the number of collapsed buildings and direct economic losses, respectively. The framework employed for these calculations is described in Silva and Horspool (2019). A comparison between the estimated and observed losses (adjusted to 2017) is depicted in Figure 10. Although a fair agreement between the estimated and observed losses was obtained (with limited bias), there is clearly a large dispersion in the results. Reasons for this variability include differences in the exposure model and the actual built environment, bias in the collection of the observed damage and losses, and large uncertainty in the ground shaking due to lack of recording stations in the affected regions (e.g. Villar-Vega and Silva, 2017).

The results from the global seismic risk model were also compared with the estimates provided by other initiatives, in particular the previously described GAR (2015) and the country profiles developed by the World Bank Group for Central America and the Caribbean (World Bank, 2017). The former risk estimates provide average annualized losses and loss exceedance curves for six building occupancies (DeBono and Chatenoux, 2015; GAR, 2015). A comparison between the aggregated *AAL* covering the residential, commercial, and industrial building stocks from GAR and this study is presented in Figure 11.

Although the AAL estimates from both studies generally agree, the results from this study are on average below the ones presented by GAR by a factor of 2. At the global scale, GAR indicates an AAL of approximately USD100 billion, while this study puts that at

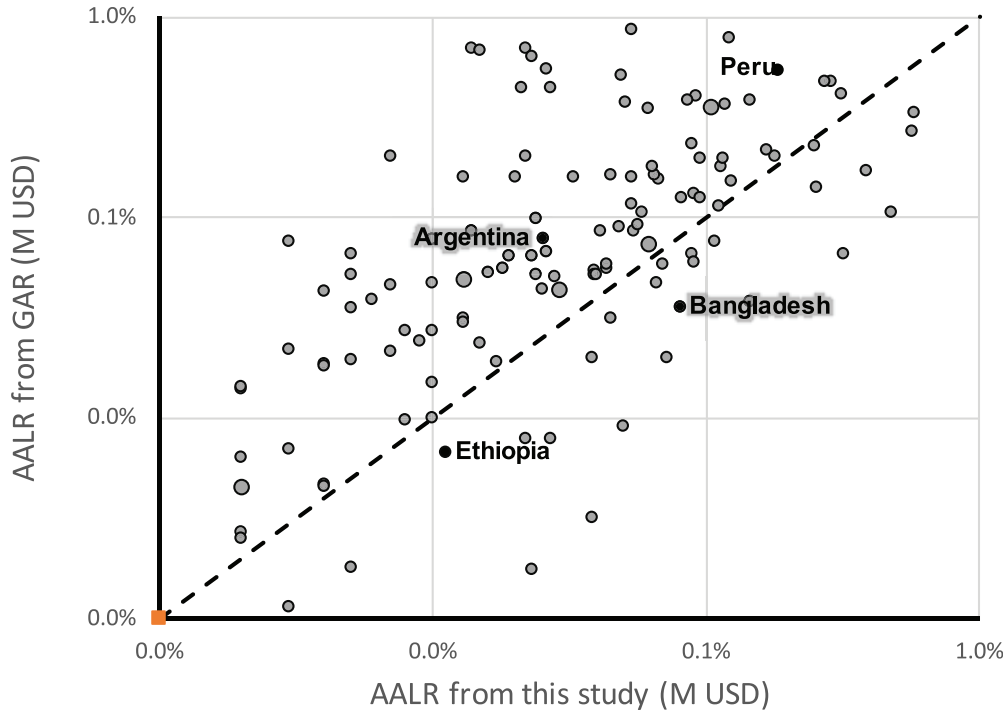


**Figure 11.** Comparison between the average annual loss (AAL) from GAR and this study.

less than half, at USD45 billion. Given the differences in the methodology to develop the exposure models between this study and GAR, it is worth also comparing the AALs normalized by the exposed value between both studies, as presented in Figure 12.

The identification of the causes for these discrepancies is a rather complex process, since as described in the preceding sections, the methodology to develop the main components (seismic hazard, exposure, and vulnerability) of GAR was considerably different. For what concerns the estimates from the World Bank Group (available through individual country profiles), the results presented herein show a strong agreement (i.e. within $\pm 20\%$), with the exception of Costa Rica. For Costa Rica, the latter study assumed rather conservative vulnerability functions, which led to high earthquake losses (Calderon and Silva, 2018).

Several comparisons with national models were also undertaken. The national seismic risk assessment for the United States published in FEMA (2017) indicates an AAL of approximately USD5.1 billion to buildings and contents (with California contributing to 61% of the annual losses), while the global model indicates an annual loss of USD4.9 billion (with California representing 66%). Despite the differences between the two risk assessment methodologies, this strong agreement with the global risk model was expected due to the use of identical exposure and seismic hazard models. For Portugal, Silva et al. (2014b) and Sousa and Campos-Costa (2015) presented an AAL of approximately EUR200 million and EUR140 million for the residential building stock, respectively. These results are 3 and 2 times higher than the annual losses provided by the global risk

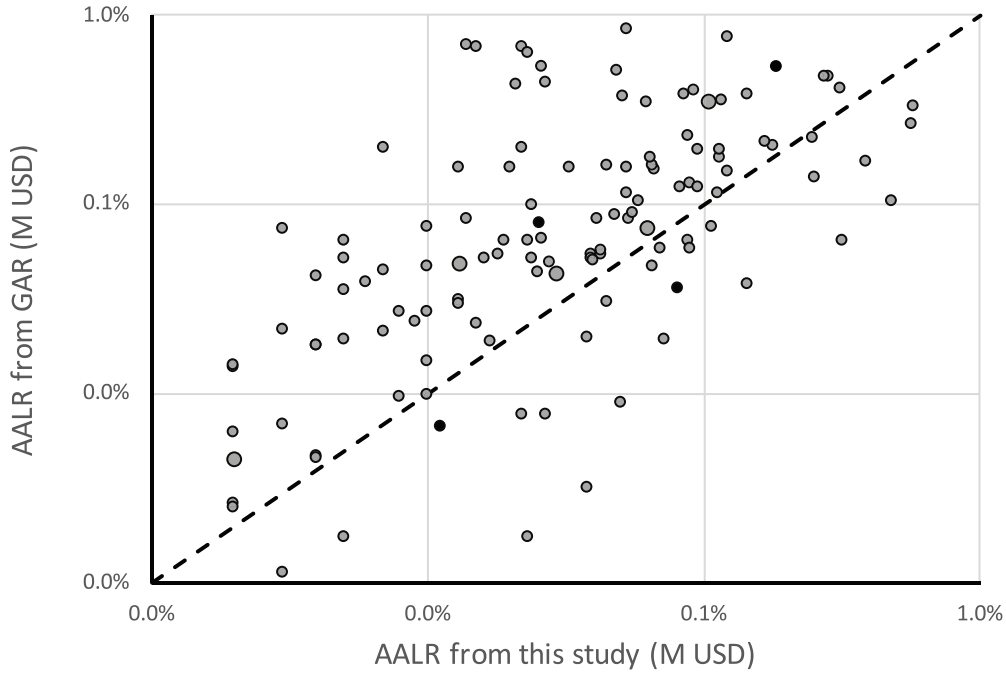


**Figure 12.** Comparison between the average annual loss ratio (AALR—in %) from GAR and this study.

model respectively. The reason for this striking discrepancy is mostly due to the differences in the seismic hazard component, as the SHARE model (used for all Europe in this study) leads to considerably lower seismic hazard in the south of the country. A similar conclusion can be drawn from the seismic risk assessment for the neighboring country of Spain performed by Salgado et al. (2015). Once again, the annual losses from the latter study are on average 2 times higher than the ones provided by the global risk model, due to the lower seismic hazard in the southern part of the country. Recently, a national multi-hazard risk assessment for Italy was coordinated by the Civil Protection Department (DPC, 2018). The latter study indicated an AAL and loss ratio for the residential building stock of USD2.3 billion and 0.67‰, while the global risk model proposes an annual loss of USD1.7 billion and loss ratio of 0.63‰. For these studies, although the same risk assessment tool was utilized (i.e. OpenQuake-engine), all three main components are distinct. These differences between the global risk model and national risk assessments strengthen the need to explore open-source tools and open-access data that allow investigating the causes behind the differences in the risk metrics.

Finally, although some of the existing disaster databases might not have sufficient events to empirically derive average annual losses, it is relevant to compare the list of the top countries in terms of observed losses with the previously presented ranking based on the *AAL* (see Figure 5). Table 1 presents the top 10 countries in terms of direct economic losses (inflation adjusted to the year of 2017) according to the disaster databases from the NatCatService (MunichRe, 2019) and the Center for Research on the Epidemiology of Disasters (CRED)'s EMDAT database (EMDAT, 2019). It is important to note that these disaster databases cover the entire built environment which include infrastructure impacts (and not just the residential, commercial and industrial buildings that are considered here),

**Table 1.** Ranking of countries based on observed losses from the NatCatService and EMDAT disaster databases and estimated *AAL* from this study and GAR.

| Ranking in terms of observed losses (1980–2017) | | Ranking in terms of the estimated *AAL* | |
|---|---|---|---|
| NatCatService | EMDAT | This study | GAR |
| Japan (22) | Japan (34) | Japan | Japan |
| China[a] (73) | China[a] (149) | China[a] | United States |
| United States (23) | Italy (25) | United States | Italy |
| Italy (13) | United States (26) | Turkey | China[a] |
| New Zealand (10) | Chile (9) | Italy | Greece |
| Chile (7) | New Zealand (5) | Mexico | Iran |
| Turkey (6) | Turkey (40) | Indonesia | Peru |
| Armenia (1) | Armenia (1) | Iran | Colombia |
| Mexico (8) | Mexico (25) | India | Chile |
| Indonesia (18) | Iran (79) | Chile | Germany |

AAL: average annual loss; EMDAT: Emergency Events Database; GAR: Global Assessment Report.
The number of events considered in the first ranking is provided in brackets.
[a]Includes Taiwan (Chinese Taipei)—GAR provides the AAL for Taiwan separately.

and the methodologies for the estimation of the economic losses are fairly different. The NatCatService relies mostly on insured losses modified by insurance penetration factors to estimate the ground-up losses. The EMDAT database is used mostly for humanitarian purposes, and thus, in some cases, it might not cover all sources of economic loss. Furthermore, unlike this study in which only the effects of ground shaking were considered, these databases also account for losses due to liquefaction, landslides, and tsunamis. The top ten countries according to the estimated $AAL$ from this study and GAR are also included in Table 1.

The comparison shown in Table 1 demonstrates a reasonable agreement between the top countries from this study and the observations from NatCat and EMDAT disaster databases, but also showcases notable differences, for example, Armenia and New Zealand rank high given the recent devastating earthquakes (M6.8 Spitak earthquake in Armenia and 2010–2011 earthquake sequence in New Zealand) witnessed in these countries.

## Conclusion

This study presented the development of a probabilistic seismic risk model at the global scale, capable of providing fundamental risk metrics such as average annualized economic losses, probability exceedance curves, or aggregated losses for specific return periods at the national or subnational level. The current model is a compilation of various country or region-specific seismic risk models, which were developed within the scope of regional programs, bilateral collaborations, or internally at the GEM Foundation. The current model indicates a global average annual economic loss of USD45 billion, and an AAL of built-up area of 64 million square meters (which is equivalent to 681 thousand dwellings lost per year in earthquakes (calculated assuming an average dwelling size of 91 $m^2$—Demographia, 2019). Japan, the United States, and China contribute almost half of the global economic losses, while every year most of the built-up area is lost in China,

Indonesia and Iran. It is worth noting that the nations with small geographic areas such as the Pacific Islands of Vanuatu and Tonga, or countries in Central America and the Caribbean like El Salvador, Nicaragua, and Haiti show high economic losses relative to their building stock value. These findings indicate that earthquake losses are likely to affect a major portion of country's economy, which could pose a serious challenge to reconstruction and recovery process in the aftermath (e.g. Haiti—DesRoches et al., 2011). The global risk results also indicate that it is the nonengineered building classes (e.g. unreinforced masonry, adobe/earthen construction) that contribute the most to the global AALs (almost 75%). Such a finding is certainly related with the fact that the vulnerable buildings continue to represent the bulk of the existing global exposure (nearly 50%), as previously mentioned.

The seismic risk estimates provided by the global model do not replace existing national risk assessments, which are likely to have a greater detail and reliability (e.g. United States—Jaiswal et al., 2015, Turkey—Bommer et al., 2002). The global seismic risk model is a dynamic model, which needs to be improved and updated continuously, as more sophisticated methodologies and data become available. The various components of the global model are expected to be released throughout 2019 and 2020, thus allowing researchers and practitioners to independently verify and validate the data and models and hopefully assist in further advancement of GEM models through community efforts. The incorporation of other phenomena such as landslides, liquefaction, and tsunamis and consideration of human and indirect losses will lead to more robust models. The authors welcome the scientific community to get involved in GEM activities and to actively collaborate in the improvement of the current global seismic risk model.

## Acknowledgments

The global seismic risk model is the result of a global collaborative effort and extensively relies on the enthusiasm and commitment of various organizations that openly collaborated with GEM and its partners. The creation of this model would not have been possible without the support provided by several public and private organizations during GEM's second working program (2014–2018). A list of the individuals that contributed to the development of the global seismic risk model can be found at www.globalquakemodel.org/risk-model-contributors. Any use of trade, firm, or product names is for descriptive purposes only and does not imply endorsement by the U.S. Government.

## Declaration of conflicting interests

The author(s) declared no potential conflicts of interest with respect to the research, authorship, and/or publication of this article.

## Funding

The author(s) received no financial support for the research, authorship, and/or publication of this article.

## References

Acevedo A, Jaramillo J, Yepes C, et al. (2017) Exploring the seismic risk of the unreinforced masonry building stock in Antioquia, Colombia. *Natural Hazards* 86(1): 31–54.

Bazzurro P and Park J (2007) The effects of portfolio manipulation on earthquake portfolio loss estimates. In: *Proceedings of the 10th international conference of application of statistics and probability in civil engineering (ICASP10)*, Tokyo, Japan, 31 July–3 August 2007.

Bommer J, Spence R, Erdik M, et al. (2002) Development of an Earthquake Loss Model for Turkish Catastrophe Insurance. *Journal of Seismology*, 6: 431–446.

Brzev S, Scawthorn C, Charleson AW, et al. (2013) *GEM building taxonomy version 2.0*. GEM Technical Report 2013-02 V1.0.0. Pavia: GEM Foundation, p. 188.

Calderon A and Silva V (2018) Probabilistic seismic risk assessment for Costa Rica. *Bulletin of Earthquake Engineering*. DOI: 10.1007/s10518-018-0499-1.

Campos Costa A, Sousa ML, Carvalho A, et al. (2010) Evaluation of seismic risk and mitigation strategies for the existing building stock: Application of LNECLoss to the metropolitan area of Lisbon. *Bulletin of Earthquake Engineering* 8: 119–134.

Cornell CA (1968) Engineering seismic risk analysis. *Bulletin of the Seismological Society of America* 58: 1583–1606.

Crowley H, Miriam C, Borzi B, et al. (2009) A comparison of seismic risk maps for Italy. *Bulletin of Earthquake Engineering* 7(1): 149–180.

Crowley H, Rodrigues D, Silva V, et al. (2018) Towards a uniform earthquake risk model for Europe. In: *Proceedings of the 16th European conference on earthquake engineering*, Thessaloniki, 18–21 June.

Dabbeek J, Silva V (2019). Modelling the residential building stock in the Middle-East for multi-hazard risk assessment. *Natural Hazards*, 10.1007/s11069-019-03842-7

Daniell JE, Khazai B, Wenzel F, et al. (2011) The CATDAT damaging earthquakes database. *Natural Hazards and Earth System Sciences* 11: 2235–2251.

Daniell JE, Schäfer AM, Wenzel F (2017). Influence of secondary hazards in earthquake loss, Frontiers in Built Environment. DOI: 10.3389/fbuil.2017.00030.

DeBono A and Chatenoux B (2015) *Global Exposure Model for GAR 2015*. Geneva: UNEP/GRID-Geneva; UNISDR.

Demographia (2019) *International House Sizes*. Available at: http://demographia.com/db-intlhouse.htm (accessed 18 March 2019).

DesRoches R, Comerio M, Eberhard M, et al. (2011) Overview of the 2010 Haiti earthquake. *Earthquake Spectra* 27(S1): 1–21.

Dolce M (2012) The Italian national seismic prevention program. In: *Proceedings of the 15th world conference on earthquake engineering*, Lisbon, 24–28 September.

DPC (2018). National risk assessment, Overview of the potential major disasters in Italy: seismic, volcanic, tsunami, hydro-geological/hydraulic and extreme weather, droughts and forest fire risks. Technical report by the Presidency of the Council of Ministers Italian Civil Protection Department, Rome, Italy.

Dunford M and Power L (2014) *National Exposure Information System (NEXIS) Building Exposure—Statistical Area Level 1 (SA1)*. Canberra, ACT, Australia: Geoscience Australia.

Elvidge CD, Baugh KE, Anderson S, et al. (2012) The night light development index (NLDI): A spatially explicit measure of human development from satellite data. *Social Geography* 7(1): 23–35.

EMDAT (2019) International Disasters Database of the Centre for Research on the Epidemiology of Disasters. Available at: https://www.emdat.be/ (accessed 3 January 2019).

Erdik M and Durukal E (2008) Earthquake risk and its mitigation in Istanbul. *Natural Hazards* 44(2): 181–197.

Federal Emergency Management Agency (FEMA) (2012) *Hazus-MH 2.1 Technical Manual: Earthquake Model*. Washington, DC: Mitigation Division, FEMA.

Federal Emergency Management Agency (FEMA) (2017) *FEMA P-366: Hazus® estimated annualized earthquake losses for the United States*. Washington, DC: FEMA.

Franco G (2015) Earthquake mitigation strategies through insurance. In Beer M, Kougioumtzoglou I, Patelli E, et al. (eds) *Encyclopedia of Earthquake Engineering*, Berlin, Heidelberg: Springer. DOI: 10.1007/978-3-642-36197-5_401-1.

Global Assessment Report (GAR) (2009) UNISDR 2009 Global Assessment Report. Available at: www.preventionweb.net/english/hyogo/gar/2009 (accessed 18 February 2019).

Global Assessment Report (GAR) (2015) UNISDR 2015 Global Assessment Report. Available at: www.preventionweb.net/english/hyogo/gar/2015 (accessed 18 February 2019).

Giardini D (1999) The global seismic hazard assessment program (GSHAP) 1992-1999: Summary volume. *Annali di Geofisica* 42(6): 957–1230.

Giardini D, Danciu L, Erdik M, et al. (2018) Seismic hazard map of the Middle East. *Bulletin of Earthquake Engineering* 16(8): 3567–3570.

Horspool N and King A (2017) What drives seismic risk in New Zealand? Insights from a next generation loss model. In: *Proceedings of the 10th pacific conference on earthquake engineering*, Sydney, NSW, Australia, 6–8 November.

Jaiswal K, Bausch D, Chen R, et al. (2015) Estimating annualized earthquake losses for the conterminous United States. *Earthquake Spectra* 31(S1): S221–S243.

Jalayer F and Cornell C (2002) Alternative nonlinear demand estimation methods for probability-based seismic assessments. *Earthquake Engineering & Structural Dynamics* 38: 951–972.

Jayaram N and Baker J (2010) Efficient sampling and data reduction techniques for probabilistic seismic lifeline risk assessment. *Earthquake Engineering and Structural Dynamics* 39(10): 1109–1131.

Kellett J and Caravani A (2013) Financing disaster risk reduction: A 20-year story of international aid. A joint report of the Global Facility for Disaster Reduction and Recovery (GFDRR) at the World Bank and the Overseas Development Institute (ODI). https://www.odi.org/sites/odi.org.uk/files/odi-assets/publications-opinion-files/8574.pdf

Kozlowski RT and Mathewson SB (1995) Measuring and managing catastrophe risk. *Journal of Actuarial Practice* 3(2): 211–241.

Lemoine A, Douglas J and Cotton F (2012) Testing the applicability of correlation between topographic slope and VS30 for Europe. *Bulletin of Seismological Society of America* 102: 2585–2599.

Li M, Zou Z, Xu G, et al. (2015) Mapping earthquake risk of the world. In: Shi P and Kasperson R (eds) *World Atlas of Natural Disaster Risk*. Dordrecht: Springer, pp. 25–39.

Lloyd C, Sorichetta A and Tatem A (2017) High resolution global gridded data for use in population studies. *Scientific Data* 4: 170001.

Martins L and Silva V (2018) A global database of vulnerability models for seismic risk assessment. In: *Proceedings of the 16th European conference on earthquake engineering*, Thessaloniki, 18–21 June.

McKenna F, Fenves G, Scott M, et al. (2000) *Open System for Earthquake Engineering Simulation (OpenSees)*. Berkeley, CA: PEER Center, University of California, Berkeley.

Mora M, Valcárcel J, Cardona O, et al. (2015) Prioritizing interventions to reduce seismic vulnerability in school facilities in Colombia. *Earthquake Spectra* 31(4): 2535–2552.

Motamed M, Calderon A, Silva V, et al. (2018) Development of a probabilistic earthquake loss model for Iran. *Bulleting of Earthquake Engineering* 17: 1795–1823.

MunichRe (2019) NatCatService—Natural catastrophe statistics online. Available at: https://natcatservice.munichre.com/ (accessed 3 February 2019).

Nath S and Thingbaijam T (2012) Probabilistic seismic hazard assessment of India. *Seismological Research Letters* 83(1): 135–149.

Ordaz M, Cardona OD, Salgado MA, et al. (2014) Probabilistic seismic hazard assessment at global level. *International Journal of Disaster Risk Reduction* 10(B): 419–427.

Pagani M, Garcia-Pelaez J, Gee R, et al. (2020) The global earthquake model (GEM) seismic hazard map. *Earthquake Spectra, in review*.

Pagani M, Hao K, Fujiwara H, et al. (2016) Appraising the PSHA earthquake source models of Japan, New Zealand, and Taiwan. *Seismological Research Letters* 87(6): 1240–1253.

Pagani M, Monelli D, Weatherill G, et al. (2014) OpenQuake engine: An open hazard (and risk) software for the global earthquake model. *Seismological Research Letters* 85(3): 692–702.

Pittore M, Haas M and Silva V (2020) Multi-resolution probabilistic modelling of residential exposure and vulnerability for seismic risk applications. *Earthquake Spectra, in review*.

Poggi V, Durrheim R, Tuluka G, et al. (2017) Assessing seismic hazard of the east African rift: A pilot study from GEM and Africa array. *Bulleting of Earthquake Engineering* 15: 4499–4529.

Pomonis A (2002) The Mount Parnitha (Athens) earthquake of September 7, 1999: A disaster management perspective. *Natural Hazards* 27: 171–199.

Romao X, Castro JM, Pereira N, et al. (2019) *European physical vulnerability models*, Deliverable 2.5 available at: http://eu-risk.eucentre.it/wp-content/uploads/2019/08/SERA_D26.5_Physical_Vulnerability.pdf

Salgado-Gálvez MA, Zuloaga-Romero D, Bernal GA, et al. (2013) Fully probabilistic seismic risk assessment considering local site effects for the portfolio of buildings in Medellín, Colombia. *Bulletin of Earthquake Engineering* 12: 671–695.

Salgado M, Cardona O, Carreño M, Barbat A (2015) Probabilistic seismic hazard and risk assessment in Spain. *Monograph Series in Earthquake Engineering* (CIMNE). MIS69, ISBN: 978-84-943307-7-3

Silva V (2017) Critical issues on probabilistic earthquake loss assessment. *Journal of Earthquake Engineering* 22: 1683–1709.

Silva V and Horspool N (2019) Combining USGS ShakeMaps and the OpenQuake-engine for damage and loss assessment. *Engineering Structures and Structural Dynamics* 48: 634–652.

Silva V, Crowley H, Pagani M, et al. (2014a) Development of the OpenQuake engine, the Global Earthquake Model's open-source software for seismic risk assessment. *Natural Hazards* 72(3): 1409–1427.

Silva V, Crowley H, Pinho R, et al. (2014b) Seismic risk assessment for mainland Portugal. *Bulletin of Earthquake Engineering* 13(2): 429–457.

Sousa M, Campos-Costa A. (2015) Evolution of earthquake losses in Portuguese residential building stock. *Bulletin of Earthquake Engineering*, 14: 2009–2029.

United Nations Office for Disaster Risk Reduction (UNISDR) (2015) *Sendai Framework for Disaster Risk Reduction*. Geneva: UNISDR.

United Nations (UN) (2016) *The Sustainable Development Goals—2030 Agenda*. Geneva: UN.

Villar-Vega M and Silva V (2017) Assessment of earthquake damage considering the characteristics of past events in South America. *Earthquake Engineering and Soil Dynamics* 99: 86–96.

Villar-Vega M, Silva V, Crowley H, et al. (2016) Development of a fragility model for the residential building stock in South America. *Earthquake Spectra* 33: 581–604.

Wald D and Allen T (2007) Topographic slope as a proxy for seismic site conditions and amplification. *Bulletin of the Seismological Society of America* 97: 1379–1395.

Wieland M, Pittore M, Parolai S, et al. (2015) A multiscale exposure model for seismic risk assessment in central Asia. *Seismological Research Letters* 86(1): 210–222.

Woessner J, Danciu L, Giardini D, et al. (2015) The 2013 European seismic hazard model—Key components and results. *Bulletin of Earthquake Engineering* 13: 3553–3596.

World Bank (2017) *Disaster Risk Profiles for Central America and the Caribbean*. Washington, DC: World Bank Group. Available at: http://documents.worldbank.org/ (accessed 9 January 2018).

Yepes-Estrada C, Silva V, D'Ayala D, et al. (2016) The global earthquake model physical vulnerability database. *Earthquake Spectra* 32(4): 2567–2585.

Yepes-Estrada C, Silva V, Valcárcel J, et al. (2017) Modelling the residential building inventory in South America for seismic risk assessment. *Earthquake Spectra* 33(2): 581–604.